

# Comparing three models of attack and failure tolerance in electric power networks

P. Hines (paul.hines@uvm.edu),  
E. Cotilla-Sanchez (eduardo.cotilla-sanchez@uvm.edu),  
S. Blumsack (blumsack@psu.edu)

July 13, 2022

## Abstract

In order to identify the extent to which results from topological graph models are useful for modeling vulnerability in power systems, we measure the susceptibility of power networks to random failures and directed attacks using three measures of vulnerability: characteristic path lengths, connectivity loss and blackout sizes. The first two are purely topological measures, following the procedure described in [1]. The blackout size calculation results from a simplified model of cascading failure in power networks. Tests with randomly selected sections of the Eastern US power grid indicate that in topological dynamics power grids are similar to random graphs, which is to be expected given the observed exponential degree distribution. However the connectivity loss model and the cascading failure model indicate that power grids behave more like scale free networks, in that they are acutely more vulnerable to directed attacks than random failures. These results suggest caution in drawing conclusions about grid vulnerability from simple topological metrics.

While the exact causes of large cascading failures are still debated, the US data indicate that their frequency is not decreasing over time [2]. Furthermore cascading failures contribute disproportionately to overall blackout risk due to the observed power-law in blackout sizes [3, 4, 2].

Motivated by the importance of reliable electricity, numerous recent papers apply methods from complex networks [5, 6] to study the structure and function of power grids. Results from these studies differ greatly. Some find exponential degree distributions [7, 1, 8], whereas others report power-law degree distributions [9, 10]. Some [1, 11] use models of the North American power grid and argue that, while the power grid differs from scale-free networks in topology, power grids are notably more vulnerable to directed attacks than random failures. Wang and Rong [12] use a topological model of cascading failure and argue that attacks on low-load nodes (buses) can have disproportionately high impact.

However, these purely topological models ignore the physical laws that govern flows in electricity networks; namely Ohm's law and Kirchhoff's laws. Some have

attempted to identify relationships between physical properties of power grids and topological metrics [13, 14, 15, 16], but to our knowledge no existing research has systematically compared the results from a cascading failure vulnerability model with those from graph theoretic models of vulnerability. In order to understand the utility of complex networks methods, such a comparison is necessary.

Thus the goal of this research is to compare the vulnerability conclusions that result from two topological measures of network vulnerability (characteristic path lengths [17] and connectivity loss [1]) with those that result from a simple model of cascading failure in power grids.

## 1 Vulnerability models

*Characteristic path length* ( $L$ , the average distance among node pairs in the giant component of a graph) was used as a measure of network vulnerability in [18]. As more components in a network fail, nodes in the giant component become more distant, which may indicate that flows within the network are inhibited.

*Connectivity loss* ( $0 < C < 1$ ) was proposed in [1] as a way to incorporate information about the connections between sources (generators) and sinks (loads) into a measure of power grid performance. If  $n_g$  is the number of generators in the network and  $n_g^i$  is the number of generators that can be reached by crossing non-failed vertices (branches) from node  $i$ ,  $C = 1 - \langle n_g^i/n_g \rangle_i$ .

The *cascading failure model* used here combines a linear approximation, known as the DC power flow, of the non-linear algebraic equations that govern flows in a power network and simple models of relays that disconnect overloaded branches. Similar models have been used to approximate cascading failures in a number of recent papers [3, 4]. While a perfect model cascading failure would accurately represent the continuous dynamics of rotating machines connected by transmission lines, the discrete dynamics associated with relays that disconnect stressed components, and the social dynamics of operators cooperating (and competing) to mitigate the effects of system stress, all models simplify these dynamics to some extent. The amount of detail necessary to accurately capture the salient properties of cascading failures is an open question [19].

In our cascading failure model we measure the result of a failure or attack by measuring the amount of load unserved at the end of the cascading failure. When a component fails, we use the DC load flow equations to compute the change in power line flows:  $P_i = \sum_j b_{ij}(\theta_i - \theta_j)$ , where  $P_i$  is the net power injected (withdrawn) from a node by generators and loads,  $\theta_i$  is the voltage phase angle at node  $i$ , and  $X_{ij}$  is the series susceptance of the branch between nodes  $i$  and  $j$ . On each branch we place a simulated time-overcurrent relay that will trip the branch if the current exceeds 50% of its rated limit for 5 seconds or more. The trip time calculations are weighted such that the relays will trip faster given greater overloads. While it is true that over-current relays are not uniformly deployed in high voltage power systems, simple

time-overcurrent relays approximate other failure mechanisms, such as lines sagging into underlying vegetation, which was an important cause of the Aug. 14, 2003 blackout [20]. After a component fails the algorithm recalculates the power flow and advances to the time at which the next component will fail, or quits if no components are overloaded. If a component failure separates the grid into unconnected sub-grids, the following process is used to re-balance load and generation. If the imbalance is small ( $<5\%$ ), generators are allowed to increase or decrease to arrive at a new supply/demand balance. If there is more than 5% excess generation, the smallest generator in the sub-grid is shut down and the re-balancing process starts over. If there is excess load after the 5% generator increase, the simulator sheds enough load to balance supply and demand. The size of the blackout is reported at the end of the simulation as the total amount of load shed by the simulator.

To estimate the impact of node failures and attacks the cascading failure model assumes that the failures occur sequentially rather than all at one time. In other words, a node failure is simulated until no overload remains, the impact computed, and then the next node failure is simulated, etc.

The aim of the simulation results that follow is essentially to identify the relationship between disturbance size and disturbance cost, using the three models of disturbance cost described above.

## 2 Attack and failure vectors

For each model described above, we estimate the impacts resulting from four failure/attack vectors. The first is random failure, in which nodes (buses) are selected for removal by random selection, with an equal failure probability for each node. The second is degree-based attack, in which nodes are removed incrementally, starting with the highest degree (connectivity) nodes. The third is load-centrality based attack, in which nodes are removed incrementally starting with nodes with the highest electrical centrality [13] with respect to load locations. The fourth is a load-quantity based attack, in which nodes are removed incrementally starting with nodes that deliver the highest quantity of load.

In *random failure* nodes are selected for removal from a uniform random distribution. This approach simulates failure resulting from natural causes (i.e., storms) at substations or an un-intelligent attack.

In *degree-based attacks* nodes are selected for removal based on their degree (the number of neighboring nodes). This strategy represents an intelligent attack, in which the attacker chooses to disable nodes with a large number of neighboring nodes.

In *load-centrality attacks*, we use the definition of electrical distance to load provided in [8] to develop an attack strategy. As in [8], we use as our measure of electrical distances the absolute value of the elements of the inverse of the system admittance matrix ( $\mathbf{Y}$ , where  $\mathbf{I} = \mathbf{Y}\mathbf{V}$  gives the relationship between nodal volt-

ages,  $\mathbf{V}$ , and net current injections,  $\mathbf{I}$ ). For a given node, we calculate the electrical distance threshold such that 90% of the total system load is reachable within that distance. Nodes are selected for removal starting with those that have the smallest electrical distance to 90% of the system load. This approach simulates an intelligent attack based on electrical data where the attacker chooses to attack nodes with high proximity to loads.

*Load-quantity attack:* Nodes are selected for removal based on the total amount of load that they deliver. This approach simulates a directed attack that is based on demand data.

The random failure, degree-based, and load-quantity attack vectors were compared in [1]. Reproducing these here allow us to compare conclusions, given a more realistic power grid model.

### 3 Results

To compare the vulnerability measures we report results from the simulation of random failures and directed attacks for a common test system (IEEE 300 bus network [21]) and 29 randomly chosen sections of the US Eastern Interconnect (EI). The EI models come from data provided by PJM for the purposes of this research. Each sub-grid is extracted from a NERC MMWG power-flow planning case by selecting a random bus in the larger network (which has approximately 50,000 nodes) and iteratively adding neighboring nodes until a network of moderate size (300-1500 buses) resulted. Of the random sub-grids generated we selected those that had an approximate balance between load and generation for further analysis. Actual locations have been deleted from our data set, such that the results are not linked to actual locations in the US power grid.

The upper panels of Figs. 3.1 and 3.2 show how path lengths ( $L$ ) change as nodes are removed from the test networks. The results are similar for both the IEEE 300 bus network, and for the EI sub-grids. Characteristic path lengths do not change substantially as the number of failed nodes increases. Directed attacks do not appear to increase path lengths in the networks any more than do random failures. This trend is similar to results reported in [18] for random graphs. We thus conclude that from a topological perspective power grids are similar to random graphs. The degree distribution of power grids is also similar to the exponential distribution found in random graphs further emphasizing the similarity.

The middle panels of Figs. 3.1 and 3.2 illustrate how connectivity loss increases as nodes are removed from the test networks, confirming results in [1], and indicating that, at least from this perspective, power grids behave similarly to scale-free networks.

The lower panels of Figs. 3.1 and 3.2 show how blackout sizes increase as nodes are removed from the test networks. Similar to the connectivity loss results, the test networks are notably more vulnerable to directed (degree-based) attacks than they

are to random failures. This is particularly clear from the averages of the 29 Eastern Interconnect sub-grids. Degree based attacks on 10 nodes produce blackouts with an average size of 80%. Random failure of 10 nodes results in an average blackout size of less than 50%. Refuting conjectures in [13], blackouts resulting from electrical-centrality based attacks are not notably larger than those that resulting from random failures.

While the results from the connectivity loss and blackout size measures are similar in trend after averaging over many simulations, the correlation among individual simulations is rather poor. Because connectivity loss does not account for cascading failure, it essentially predicts only the minimum size of the resulting failure (see Fig. 3.3). In many cases the actual impact of the attack is greatly amplified through the cascading failure process.

## 4 Conclusions

The results described in this paper indicate that simple topological measures of power grid vulnerability produce very different results from those that account for the physical laws that govern flows in power grids (Ohm's law and Kirchhoff's laws), as well as the locations of power sources and sinks. When measuring the impact of a sequence of node failures with characteristic path lengths, power grids appear to be fairly resilient to both random failure and directed attack. These results emphasize that power grid topology is similar to that of random graphs, and is consistent with results reported in [1]. However, when impact (or cost) is measured using cascading failure size, with the amount of load lost as the measure of size, power grids appear to be significantly more vulnerable to directed attacks than random failures. This is similar to topological results obtained for scale free networks [18]. We conclude that the electrical structure of power grids is dramatically different from their topological structure, and that power system vulnerability results that are based purely on topological models can be misleading.

If the DC models that we present here correlate to what would obtain from a more sophisticated model of cascading failure, the overall implication is that the protection of high-degree substations (ones with a high number of transmission lines to other substations) from attack may be a cost-effective risk mitigation strategy.

## Acknowledgement

This work is supported in part by the US National Science Foundation (Award #0848247) and in part by PJM Interconnection.

## References

- [1] R. Albert, I. Albert, and G. Nakarado, “Structural vulnerability of the north american power grid,” *Physical Review E*, vol. 69, no. 2, FEB 2004.
- [2] P. Hines, J. Apt, and S. Talukdar, “Large blackouts in north america: Historical trends and policy implications,” *Energy Policy*, (*In press*), 2009.
- [3] B. A. Carreras, D. E. Newman, I. Dobson, and A. B. Poole, “Evidence for Self-Organized Criticality in a Time Series of Electric Power System Blackouts,” *IEEE Transactions on Circuits and Systems–I: Regular Papers*, vol. 51, no. 9, pp. 1733–1740, 2004.
- [4] I. Dobson, B. Carreras, V. Lynch, and D. Newman, “Complex systems analysis of series of blackouts: cascading failure, critical points, and self-organization,” *Chaos: An Interdisciplinary Journal of Nonlinear Science*, vol. 17, p. 026103, 2007.
- [5] R. Albert and A. Barabasi, “Statistical mechanics of complex networks,” *Reviews of Modern Physics*, vol. 74, 2002.
- [6] S. Boccaletti, V. Latora, Y. Moreno, M. Chavez, and D.-U. Hwang, “Complex networks: Structure and dynamics,” *Physics Reports*, no. 424, pp. 175–308, 2006.
- [7] L. A. N. Amaral, A. Scala, M. Barthelemy, and H. E. Stanley, “Classes of small-world networks,” *Proceedings of the National Academies of Science*, vol. 97, no. 21, pp. 11 149–11 152, Apr 2000.
- [8] P. Hines, S. Blumsack, E. C. Sanchez, and C. Barrows, “The topological and electrical structure of power grids,” in *Proceedings of the 43rd Hawaii International Conference on System Sciences (forthcoming)*, 2010.
- [9] A.-L. Barabasi and R. Albert, “Emergence of scaling in random networks,” *Science*, vol. 286, pp. 509–512, 1999.
- [10] D. Chassin and C. Posse, “Evaluating north american electric grid reliability using the barabasi-albert network model,” *Physica A*, vol. 355, pp. 667 – 677, 2005.
- [11] Å. J. Holmgren, “Using graph models to analyze the vulnerability of electric power networks,” *Risk Analysis*, vol. 26, no. 4, pp. 955 – 969, Sep 2006.
- [12] Z. Wang, R. J. Thomas, and A. Scaglione, “Generating random topology power grids,” in *Proceedings of the 41st Hawaii International Conference on System Sciences*, 2008.

- [13] P. Hines and S. Blumsack, "A centrality measure for electrical networks," *Proceedings of the 41st. Hawaii International Conference on System Sciences*, 2008.
- [14] S. Arianos, E. Bompard, A. Carbone, and F. Xue, "Power grids vulnerability: a complex network approach," *Chaos*, vol. 19, 2009.
- [15] E. Bompard, R. Napoli, and F. Xue, "Analysis of structural vulnerabilities in power transmission grids," *International Journal of Critical Infrastructure Protection*, 2009.
- [16] R. Sole, M. Rosas-Casals, B. Corominas-Murtra, and S. Valverde, "Robustness of the european power grids under intentional attack," *Physical Review E*, vol. 77, 2008.
- [17] D. J. Watts and S. H. Strogatz, "Collective dynamics of 'small-world' networks," *Nature*, vol. 393, pp. 440–442, 1998.
- [18] R. Albert, H. Jeong, and A.-L. Barabasi, "Error and attack tolerance of complex networks," *Nature*, vol. 406, pp. 378–382, 2000.
- [19] R. Baldick, B. Chowdhury, I. Dobson, Z. Dong, B. Gou, D. Hawkins, H. Huang, M. Joung, D. Kirschen, F. Li, J. Li, Z. Li, C.-C. Liu, L. Mili, S. Miller, R. Podmore, K. Schneider, K. Sun, D. Wang, Z. Wu, P. Zhang, W. Zhang, and X. Zhang, "Initial review of methods for cascading failure analysis in electric power transmission systems ieeepes task force on understanding, prediction, mitigation and restoration of cascading failures," in *IEEE Power and Energy Society General Meeting*, July 2008.
- [20] USCA, "Final Report on the August 14, 2003 Blackout in the United States and Canada," US-Canada Power System Outage Task Force, Tech. Rep., 2004.
- [21] PSTCA. (2007) Power Systems Test Case Archive, University of Washington, Electrical Engineering. online: <http://www.ee.washington.edu/research/pstca/>. [Online]. Available: <http://www.ee.washington.edu/research/pstca/>

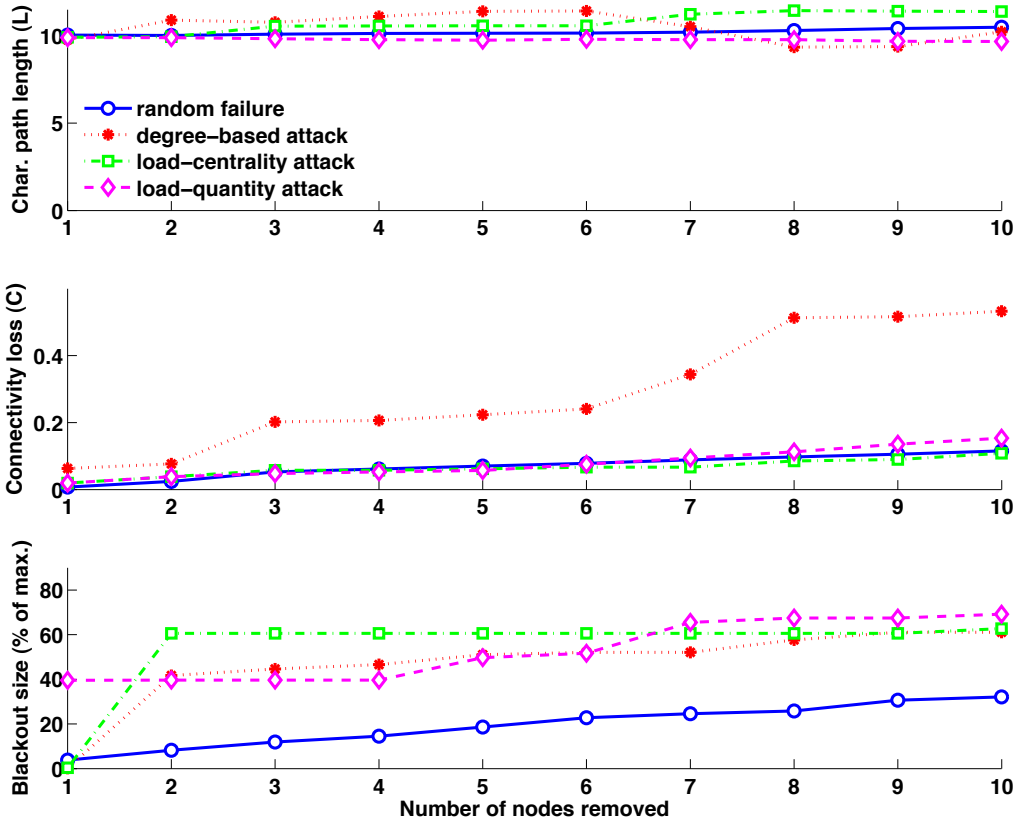


Figure 3.1: (color online). Simulated response of the IEEE 300 bus network to random failures and directed attacks. The top panel shows the change in network size (characteristic path lengths,  $L$ ) as the number of failures increases. The middle panel shows the increment on connectivity loss ( $C$ ) as the number of failures increases. The bottom panel shows the size of the resulting blackout (from the DC model described in Section 2) as a function of the number of components failed. The results for random failures are averages over 10 iterations.

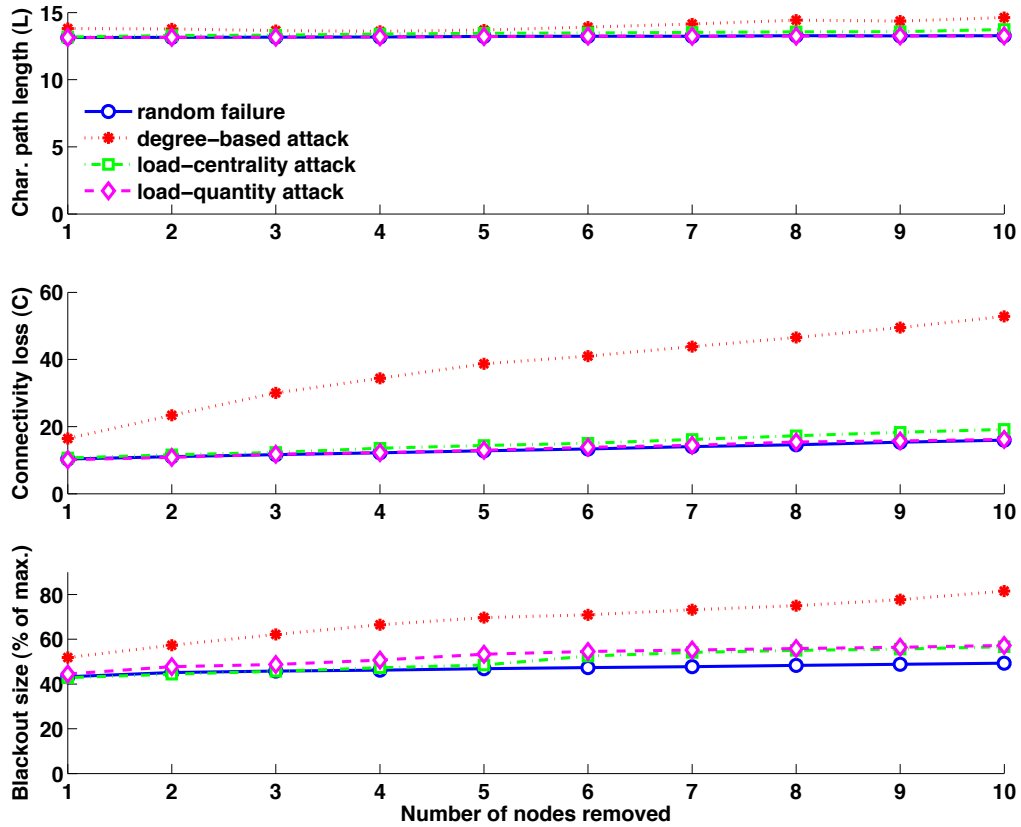


Figure 3.2: (color online). Simulated response of 29 portions of the Eastern Interconnect network to random failures and directed attacks. The top panel shows the average network size (characteristic path lengths,  $L$ ) as the number of failures increases. The middle panel shows the increment on connectivity loss ( $C$ ) as the number of failures increases. The bottom panel shows the size of the resulting blackout (from the DC model described in Section 2) as a function of the number of components failed. Each data point represents an average value over all model runs.

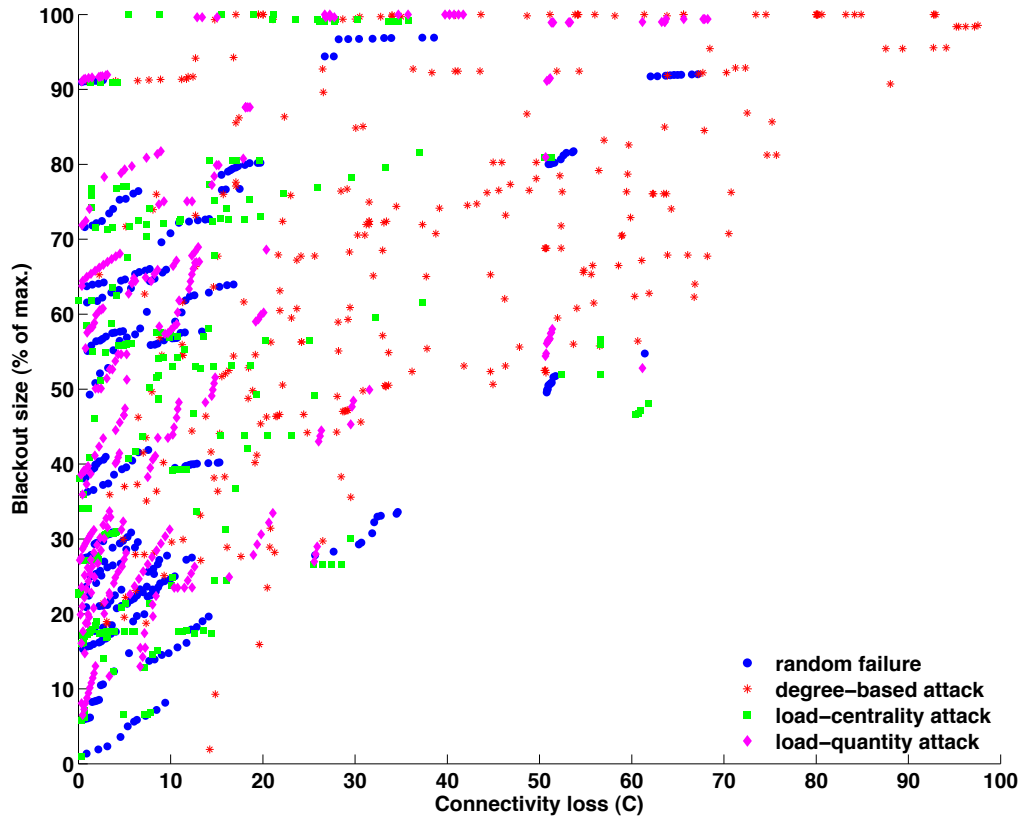


Figure 3.3: (color online). The correlation between blackout sizes and connectivity loss ( $C$ ) for 29 portions of the Eastern Interconnect network. The correlation coefficients corresponding to each attack vectors are as follow:  $\rho = 0.4539$  (random failure),  $\rho = 0.5677$  (degree-based attack),  $\rho = 0.3251$  (load-centrality attack),  $\rho = 0.5391$  (load-quantity attack). The aggregated correlation coefficient is  $\rho = 0.5324$ .